

COMPUTER-AIDED DESIGN OPTIMIZATION OF CATALYTIC EXHAUST TREATMENT SYSTEMS FOR GASOLINE-POWERED CARS

George Konstantas and Anastassios Stamatelos

University of Thessaly, Mechanical Engineering Department,
Laboratory of Thermodynamics & Thermal Engines
Pedion Areos, 383 34 Volos, Greece
Email: stam@uth.gr

ABSTRACT

Stringent legislation on vehicles' emissions levels worldwide, is a significant driving force for automotive manufacturers to develop increasingly complex exhaust treatment systems. Gasoline engine improvements during the last decade, including the introduction of gasoline direct injection (lean burn engines with increased part-load efficiency) necessitate the introduction of additional catalytic exhaust treatment devices (NO_x traps, etc.) that must be optimized in parallel with the standard three-way catalytic converters for stoichiometric engines. Optimal design includes both engine management (lambda, engine-out temperature, cold-start operation, etc.) and design parameters of the exhaust treatment device. This paper focuses on the computer-aided optimization of standard three-way catalytic converter systems. However, the optimization methodologies and computational tools described here are also applicable to exhaust treatment systems for gasoline direct injection and Diesel engines.

1 INTRODUCTION

Catalytic converters have been extensively studied and continuously improved over the past 30 years. Advances in materials, design and washcoat formulations resulted in advanced systems, with numerous engine management implications. Mathematical modeling is widely applied today in the design optimization of this type of systems [1][2]. The models in use are successfully describing the most prominent physical and chemical phenomena taking place inside the converter. Of course, high Precious Metal loading usually leads to the achievement of higher activity and durability of catalytic converters. However, the necessity to maintain the cost of the final product at acceptable levels, places additional, difficult – to - satisfy, constraints to the designer. A remarkable question refers to the optimized combination of precious metals and oxygen storage components loading and converter geometrical characteristics. Mathematical modeling seems to have reached by now, an adequate level of capacity to support the designer in this type of tasks, as will be demonstrated in this paper.

Despite the variety of modelling approaches in use today, the majority of them share a common structure, which is dictated by the structure and operating concept of the catalytic converter itself, which is essentially a batch of parallel channels, impregnated by a chemically active washcoat layer. Thus, each modelling approach must address three distinct levels:

washcoat level: At this level, local phenomena at each point of the washcoat along the channel axis are considered. Two dominant phenomena must be modelled: diffusion and simultaneous reaction within the washcoat.

channel level: At this level, the local information provided by the washcoat model is exploited, to determine the mass and heat transfer between the exhaust gas and the solid phase (substrate and washcoat) and consequently, the exhaust gas characteristics (temperature and species concentrations) along the channel. At this level, chemical and physical phenomena in the washcoat are viewed as heat or mass sinks/sources. Profiles of concentration and convective heat transfer between the channel wall and the gas are computed along the channel axis

reactor level: At the reactor level, the channel-level information is exploited, to compute heat transfer interaction between channels. At this level, the heat sources computed for each channel at the kinetics and channel level calculations are used to estimate the temperature field of the monolith. Heat transfer calculations vary from 1-D to 3-D. 1D reactor level models treat all the channels of the monolith identically, 2D models divide the monolith into sectors (clusters of channels) and the channel level computations are done for each one of the distinct sectors [3]. Finite-volume or finite element approaches may be employed in the 3D computation (e.g. [4],[5]).

At the washcoat level, every model includes a chemical reaction kinetics submodel, which employs a number of tunable kinetic parameters to successfully match the complex catalytic reaction behaviour [6]. This happens because each washcoat formulation has a different, complex chemical activity in the various reactions and reactor conditions. In the past, tuning of the kinetics parameters was based on a manual, empirical procedure. The advent of advanced optimization techniques makes today possible to obtain good predictions of the transient performance during the legislated tests (NEDC, FTP-75 etc) with reduced reaction schemes [7]. Of course, good predictions are only possible when an adequate quality assurance system is established for the experimental data employed in the simulations and validation studies [8]. In what follows, we start with a brief presentation of our modelling approach,

that combines an updated version of the catalytic converter modelling software [9] with optimisation tools, tailored to the computer-aided estimation of the model's chemical kinetics parameters. The details of the developed optimisation methodology have already been presented elsewhere [7]. Here we demonstrate its application to some interesting design optimisation case studies.

2 MATHEMATICAL MODELING APPROACH

Washcoat level modelling

A ‘‘film model’’ approach, (e.g [10][11]), approximates the washcoat with a solid–gas interface, where it is assumed that all reactions occur. This approximation essentially neglects diffusion effects in the pore system of the washcoat and assumes that all catalytically active sites are directly available to gaseous-phase species at this solid–gas interface:

$$\frac{\rho_g}{M_g} k_{m,j} S (c_j - c_{j,s}) = R_j \quad (1)$$

On the right hand side of (1), the rate R_j refers to the production or consumption of each species at the solid–gas interface. For N_R reactions, each taking place with a rate r_k , the rate of consumption or production of a species j is:

$$R_{rea,j} = \delta \gamma S \sum_{k=1}^{N_R} (a_{j,k} r_k) \quad (2)$$

where $a_{j,k}$ is the stoichiometric coefficient of species j in reaction k , δ is the washcoat thickness and γ is the specific catalyst area, i.e. catalytically active area per washcoat volume.

The two primary categories of heterogeneous catalytic reactions occurring in the washcoat, are reduction-oxidation (redox) reactions and oxygen storage reactions (see reaction scheme in Table 1). Oxygen storage phenomena play a principal role in the efficiency of the modern three-way catalytic converter, as they supply the lack of oxygen under reducing environment. Oxygen storage occurs mainly on the Ceria (Ce) surface, which is contained in large quantities in the catalyst's washcoat (at the order of 30% wt). Under net oxidizing conditions, 3-valent Ce oxide (Ce_2O_3) may react with O_2 or NO and oxidize to its 4-valent state (CeO_2). Under net reducing conditions, CeO_2 may function as an oxidizing agent for CO , HC and H_2 .

The model uses the auxiliary quantity ψ to express the fractional extent of oxidation of the oxygen storage component. Specifically, the oxidation rate of the oxygen storage component is assumed proportional to the active sites of Ce_2O_3 , i.e. to $\Psi_{cap}(1-\psi)$. On the other hand, the oxidation rate of CO and HC by CeO_2 is assumed proportional to $(\Psi_{cap} \psi)$. Moreover, the rates of these reactions should be linearly dependent on the local concentration of the corresponding gaseous phase reactant.

The rate of variation of ψ is the difference between the rate that Ce_2O_3 is oxidized and reduced:

$$\frac{d\psi}{dt} = -\frac{r_6 + r_7}{\Psi_{cap}} + \frac{r_8 + r_9}{\Psi_{cap}} \quad (3)$$

Equation (4) is solved analytically for ψ at each node along the catalyst channels. According to Table 1, the model employed in this study includes a minimized set of 9 apparent reactions with 8 tunable parameters. The kinetics of H_2 oxidation are assumed equal to those of CO oxidation, in line with experience and the original kinetic parameters published by Voltz [12]. A justification for this assumption is that in presence of CO the oxidation rate of hydrogen is inhibited by CO to approximately the same extent as the oxidation of CO itself [13].

Channel level modelling

For the formulation of the channel-level model, two usual simplifications are employed [14],[10], namely: (i) The axial diffusion of mass and heat in the gas phase is negligible (ii) The mass and heat accumulation in the gas phase is negligible. (This includes the assumption for the quasi-steady state nature of the problem.)

Using the quasi-steady state approximation and neglecting diffusion and accumulation terms, the mass balance for the gas phase becomes:

$$\rho_g u_z \frac{\partial c_j(z)}{\partial z} = \rho_g k_{m,j} S (c_j(z) - c_{s,j}(z)) \quad (4)$$

where c_j is a mean bulk value employed for the gas–phase concentration of each species and $c_{s,j}$ the respective one at the solid-gas interface. Energy is transferred to and from the exhaust gas only due to convection with the channel walls (gas-phase energy balance):

$$\rho_s c_p u_z \frac{\partial T_g(z)}{\partial z} = h S (T_s(z) - T_g(z)) \quad (5)$$

Similarly to the above, a mean bulk value T_g is used for the exhaust gas temperature, and a solid phase temperature T_s is introduced for the monolith and the solid–gas interface. Parameter h is the heat transfer coefficient and is calculated as a function of the Nusselt number. Finally, the boundary conditions for the temperature, mass flow rate and concentrations are given from measurement at the converter’s inlet:

Reactor level modelling

The reactor model presented in this work is a one-dimensional heat transfer model for the transient heat conduction in the monolith. Heat losses to the environment via convection and radiation are also taken into account. The model’s primary assumptions are the following:

The temperature field in the converter is described by the equation of transient heat conduction in one-dimension, with heat sources being convection from the exhaust gas, the enthalpy released from the reactions and convection to ambient air.

$$\rho_s c_{p,s} \frac{\partial T_s}{\partial t} = k_{s,z} \frac{\partial^2 T_s}{\partial z^2} + hS(T_g - T_s) + \sum_{k=1}^{N_R} (-\Delta H_k) r_k + Q_{amb} \quad (6)$$

Finally, the boundary condition needed for the solution of the heat conduction equation refers to the heat losses to ambient air:

$$Q_{amb} = S_{mon} [h_{amb}(T_s - T_{amb}) + \varepsilon\sigma(T_s^4 - T_{amb}^4)] \quad (7)$$

Table 1 Reaction scheme and rate expressions of the model

		Reaction	Rate expression
Reduction - Oxidation reactions	1	$\text{CO} + \frac{1}{2}\text{O}_2 \longrightarrow \text{CO}_2$	$r_1 = \frac{A_1 e^{-E_1/R_g T} c_{\text{CO}} c_{\text{O}_2}}{G}$
	2	$\text{H}_2 + \frac{1}{2}\text{O}_2 \longrightarrow \text{H}_2\text{O}$	$r_2 = \frac{A_2 e^{-E_2/R_g T} c_{\text{H}_2} c_{\text{O}_2}}{G}$
	3, 4	$\text{C}_\alpha \text{H}_\beta + (\alpha + 0.25\beta)\text{O}_2 \longrightarrow \alpha \text{CO}_2 + 0.5\beta \text{H}_2\text{O}$	$r_k = \frac{A_k e^{-E_k/R_g T} c_{\text{C}_\alpha \text{H}_\beta} c_{\text{O}_2}}{G}, k = 3, 4$
	5	$2\text{CO} + 2\text{NO} \longrightarrow 2\text{CO}_2 + \text{N}_2$	$r_5 = A_5 e^{-E_5/R_g T} c_{\text{CO}} c_{\text{NO}}$
	Oxygen storage reactions	6	$2\text{CeO}_2 + \text{CO} \longrightarrow \text{Ce}_2\text{O}_3 + \text{CO}_2$
7		$\text{C}_\alpha \text{H}_\beta + (2\alpha + \beta)\text{CeO}_2 \longrightarrow (\alpha + 0.5\beta)\text{Ce}_2\text{O}_3 + \alpha \text{CO}_2 + 0.5\beta \text{H}_2$	$r_7 = A_7 e^{-E_7/R_g T} c_{\text{C}_\alpha \text{H}_\beta} \Psi \Psi_{cap}$
8		$\text{Ce}_2\text{O}_3 + \frac{1}{2}\text{O}_2 \longrightarrow 2\text{CeO}_2$	$r_8 = A_8 e^{-E_8/R_g T} c_{\text{O}_2} (1 - \Psi) \Psi_{cap}$
9		$\text{Ce}_2\text{O}_3 + \text{NO} \longrightarrow 2\text{CeO}_2 + \frac{1}{2}\text{N}_2$	$r_9 = A_9 e^{-E_9/R_g T} c_{\text{NO}} (1 - \Psi) \Psi_{cap}$
Inhibition term		$G = T(1 + K_1 c_{\text{CO}} + K_2 c_{\text{CxHy}})^2 (1 + K_3 c_{\text{CO}}^2 c_{\text{CxHy}}^2) (1 + K_4 c_{\text{NO}}^{0.7}), K_i = k_i \exp(-E_i/R_g T)$	

Kinetic Parameter Estimation Methodology

The kinetics submodel introduces into the catalytic converter model a set of parameters that have to be estimated with reference to a set of experimental data. Tunable parameters take into account the reactivity of the specific washcoat formulation as well as any other aspect of catalytic converter operation that is not included in the model explicitly. In the present model, the tunable parameters are the activation energy E_k and the pre-exponential factor A_k that are included in the reaction rate r_k of each reaction k . The values of activation energies are more or less known from Arrhenius plots [12], [15], [16] and only the pre-exponential factors are tuned (8 tunable parameters). Apart from reaction activity, approximations that have been done during model formulation, like the effect of reaction scheme and rate expressions simplifications, the effect of exhaust gas input data uncertainty and simplifications (fast and slow hydrocarbons, NO), the effect of neglect of diffusion through the pore system of

the washcoat, are lumped in the tunable parameters. In the present work a genetic algorithm is applied as an optimisation methodology [17],[18] for kinetic tuning.

Formulation of the performance measure

A performance measure is defined that exploits the information of species concentrations measurements at the inlet and the outlet of the catalytic converter, from a second-by-second (or faster acquisition) data file recorded from a legislated test cycle (NEDC, FTP-75 etc). Specifically, it is based on the conversion efficiency ε_j for a pollutant j . Herein, we take into account the three legislated pollutants, thus $j = \text{CO}, \text{HC}, \text{NO}_x$. To account for the goodness of computation results compared with a measurement that spans over a certain time period, an error e for each time instance must be defined. The latter should give the deviation between computation and measurement for the conversion efficiency ε . Summation over time should then be performed to calculate an overall error value for the whole extent of the measurement. Here, the error is defined as:

$$|e| = |\varepsilon - \hat{\varepsilon}|. \quad (8)$$

A quantity e_{\max} is the maximum error between computation and measurement, and it is defined as

$$e_{\max}(t_n) = \max\{\hat{\varepsilon}(t_n), 1 - \hat{\varepsilon}(t_n)\} \quad (9)$$

In this work, we define the performance measure F as the mean value of the error to maximum error over the time period of interest:

$$F(\mathcal{G}) = \frac{1}{N} \sum_{n=0}^N \frac{|e(t_n; \mathcal{G})|}{e_{\max}(t_n)} \quad (10)$$

The performance measure defined in (10) is used for the assessment of the performance of each of the three pollutants CO, HC, NO_x. The total performance measure is computed as the mean of these three values.

Optimization procedure

Having defined the performance measure for the model, the problem of tunable parameter estimation reduces in finding a tunable parameter vector \mathcal{G} that maximizes F , expressed as:

$$\text{Maximize } F'(\tilde{\mathcal{G}}) = 1 - F(\tilde{\mathcal{G}}) = \frac{1}{3N} \sum_{j=\text{CO,HC,NO}_x} \sum_{n=0}^N \frac{|e_j(t_n; \tilde{\mathcal{G}})|}{e_{j,\max}(t_n)}, \quad N = \tau/\Delta t \quad (11)$$

This is a constraint maximization problem, since the components of vector \mathcal{G} are allowed to vary between two extreme values, i.e. $\mathcal{G}_{i,\min} \leq \mathcal{G}_i \leq \mathcal{G}_{i,\max}$. Here, a genetic algorithm has been employed for the maximization of (11). The randomized nature of the genetic algorithm enables it to avoid local extrema of the parameter space and converge towards the optimum or a near-optimum solution. It should be noted, though, that this feature does not guarantee convergence to the global optimum. This behaviour is common to all multimodal optimization techniques and not a specific genetic algorithm characteristic.

The implementation of the genetic algorithm that was described above is not the only one possible. There are a number of design decisions and parameters that influence the operation, efficiency and speed of the genetic algorithm. The present implementation of genetic algorithm includes a subroutine for examining multiple local extrema that constricts the convergence of the whole population near a solution by selecting a small portion of solutions biased towards the less fit individuals. Its characteristics are summarized in Table 2.

Table 2 Parameters of the genetic algorithm

Encoding type	binary
Crossover operator	one-point crossover
Population size	60
Crossover probability	0.6
Encoding resolution	10 bit

Once the CATRAN code is tuned to describe the performance of a reference catalyst formulation, it may be employed in design optimization studies, involving optimal selection of several design parameters, e.g. catalytic converter dimensions, cell density versus wall thickness / washcoat loading, precious metal – versus ceria loading. In the past, most of the above design optimization studies are carried out manually (e.g. [19] [20]). Today, modern optimization tools (genetic algorithms), combined with a reduced number of laboratory tests, start to be employed in the computer-aided optimization of certain design parameters (mainly precious metal loading and Ceria loading).

3 ENGINEERING DESIGN APPROACH

The design strategy of catalytic converters is a cyclic procedure [21] that can take place at many different levels of complexity assisted by experiments and modelling. The most fundamental level corresponds to the study of washcoat processes and the full scale level studies the overall performance of the final product. The approach described in this paper studies and simulates full-scale engine tests, assisting the engineering design of the final product, but also, at the same time, giving feedback to the fundamental level referenced above. At the full-scale level, due to the overall system complexity, a quality assurance methodology is essential for a systematic study of experimental data. The transient operation of the engine, lambda oscillations and the associated variations in exhaust gas composition, limitations of instrumentation measurability and different instrumentation measuring responses affect the desirable quality of experimental data. The use of low quality experimental data can drive to misunderstanding of coupled phenomena inside the converter and possibly misleading design suggestions [8]. Moreover, the simulation models must be fast enough for engineering design optimization (significantly faster than realtime). On the other hand, fundamental level catalyst experiments (e.g. [22]), can only be fitted with complex elementary reaction schemes, with a complicated tuning procedure. However, the tuning is useless if we shift even to a slightly different catalyst – washcoat formulation or even loading.

Thus, it is preferable to minimize as much as possible the reaction scheme in order to gain the full control of the model and uncouple somehow the chemical reactions. Primary and secondary effects inside the catalytic converter must be studied and weighted respectively to the contribution they have in the overall performance of the converter.

A schematic representation of the overall approach of the case of 3 way catalytic converters modeling can be summed up to the Figure 1. It should be mentioned here that the increasingly stringent standards for automobile tailpipe emissions geometrically increase the required prediction accuracy. An engineering design approach is attached basically at full-scale level modeling and engine experiments presented in Figure 1. Simplified approaches of the chemical phenomena inside the converter with the use of minimized reaction schemes with tunable apparent kinetic expressions [7],[23],[24], assume that each washcoat formulation can be considered as a “black box” with different, complex activity in the various reactions and reactor conditions. This approach is proven to give good predictions of the overall behavior of the catalyst under real engine conditions on legislated driving cycles. Once a specific washcoat behavior from a reference catalyst is fitted it may be employed either on different driving patterns or in design parameters optimization studies.

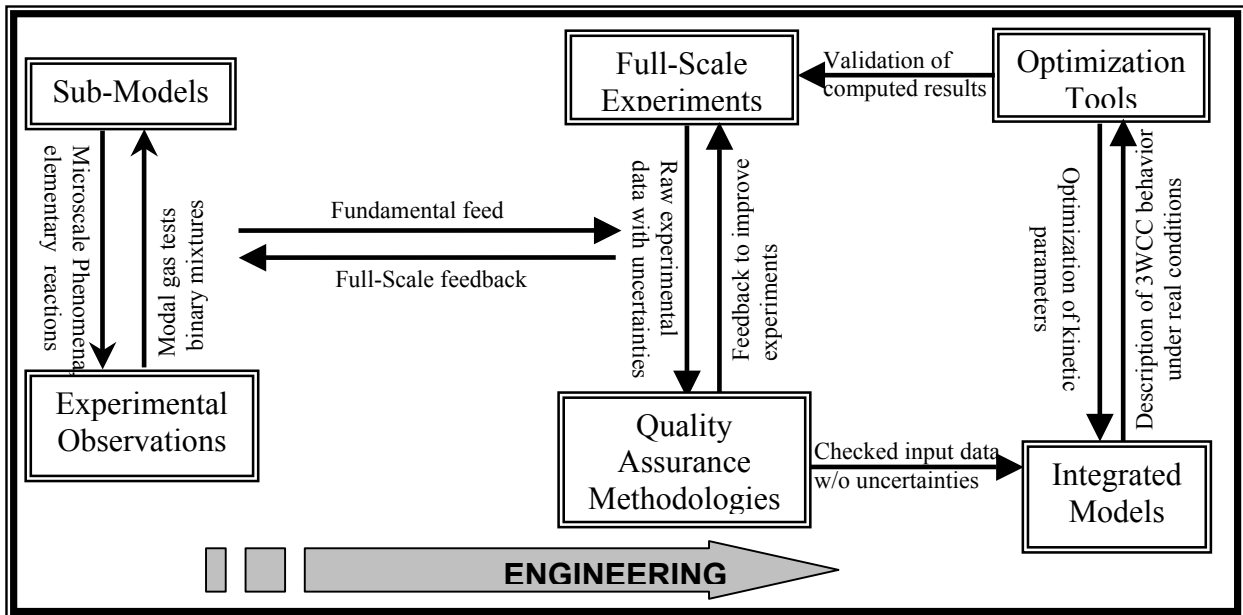


Figure 1 Schematic representation of the 3WCC design strategy with the coupling of experiments and modelling at two levels of study

4 DEFINITION OF DESIGN OPTIMIZATION CASE STUDY

In this paper, the catalyst model’s kinetic parameters are tuned to fit the behavior of four reference catalysts of equal size, (2.4 l.), loaded with 10, 30, 50, 100 g/ft³ precious metal respectively, 7:1 Pt to Rh ratio, installed on a 2 liter displacement SI engine. The catalytic converters have a similar washcoat formulation and loading, and their behavior is tested on the chassis dynamometer, according to the NEDC legislated cycle. The main objective is to check the model’s accuracy and predictive ability, and possibly draw a correlation of the kinetic performance of each converter with its respective Precious Metal Loading level.

The importance of this study is associated with the fact that although several design parameters of the catalyst are known or are easily calculated (dimensions, insulation and substrate physical properties), washcoat composition

and preparation are valuable trade secrets covered by industrial secrecy. For example, the real oxygen storage capacity of a catalytic converter is a function primarily of ceria added to the washcoat and the percentage thereof that is active and secondarily of the ability of precious metals to store oxygen. Estimation of this complex behavior can be based on specially designed dynamic tests (e.g. [25]), but also by fitting of the catalyst's oxygen storage and release behaviour in legislated driving cycles using a computational model. The fitting of catalyst oxygen out curves ensures a good estimation of the real oxygen storage capacity of the converter and a good prediction of the filling rate of oxygen storage. As expected, the engine out emissions of the specific engine, are subject to a reasonable statistical variation [26], as shown in the first column of Table 3, also compared to oncoming EU and US standards. The differences in their performance can be attributed to different engine out emissions, but essentially to the activity of their washcoats.

Table 3 Engine-out and tailpipe emissions for the specific engine and 3WCC combinations

	<i>Engine out</i>	<i>Euro 4</i>	<i>ULEV</i>	<i>10g/ft³</i>	<i>30g/ft³</i>	<i>50g/ft³</i>	<i>100g/ft³</i>
<i>CO (g/km)</i>	7.0 – 7.6	1.0	1.0	1.86	1.39	1.17	1.29
<i>HC (g/km) (C1)</i>	1.7 - 2	0.1	0.028	0.3	0.25	0.21	0.22
<i>NOx (g/km)</i>	2.8 - 3	0.08	0.117	0.1	0.076	0.065	0.06

As a second step, a simple catalytic converter length optimization study is carried out with the more standard, 50g/ft³ formulation. The objective is to reduce the converter length, based on the reference one, to conform to less demanding overall CO, HC and NOx emissions values. An experimental validation of the result is made by use of an additional experimental determination of the performance of a shorter catalytic converter installed on the same engine.

5 KINETIC TUNING OF THE 10 g/ft³ CATALYST

The less active catalyst (10g/ft³) is selected for the first tuning with the genetic algorithm tool. The kinetic parameters of the model were tuned with a genetic algorithm tool for 100 generations of 60 individuals. The comparison of computed to the corresponding measured cumulative as well as instantaneous emissions curves are presented in Figure 2 -

Figure 5 and show a good fit between the model and the real behavior of the 3WCC.

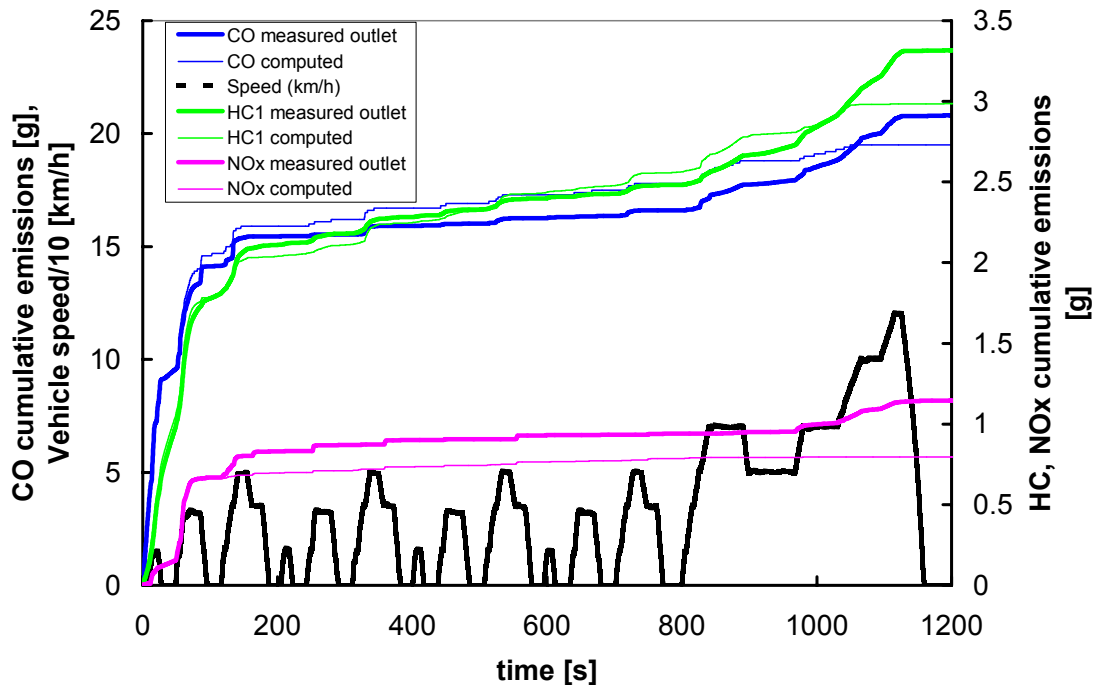


Figure 2 Measured versus computed cumulative tailpipe emissions for the case of 10g/ft³ PML catalyst on NEDC. Bold lines: measured, thin lines: computed

The model captures the light-off behavior and the cumulative emissions curves are very close to the experimental ones. The model seems to lose some accuracy at the end of the driving cycle (extra-urban part), where increased converter temperatures prevail. The period 0 - 600 s is selected as the most representative area for the instantaneous tailpipe emissions as it includes the performance of the catalytic converter during cold start (0 - 195s)

and urban driving pattern (195-600s). Especially, during the cold start period the catalytic converter is initially inactive and gradually activates as it is heated up by exhaust gas heat convection and heat released by the exothermic reactions taking place.

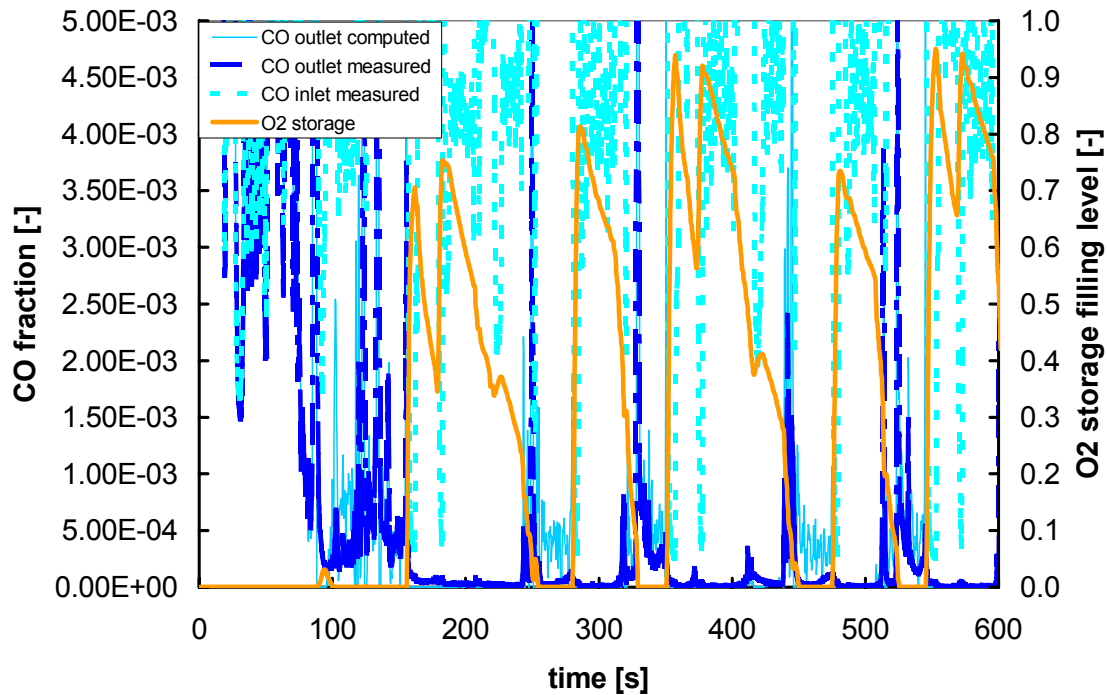


Figure 3 Measured versus computed instantaneous tailpipe CO emissions for the case of 10g/ft³ PML catalyst on NEDC. Bold lines: measured, thin lines: computed

Apparently, the model successfully matches the light-off behaviour of the catalyst, as well as subsequent breakthroughs during acceleration. The role of oxygen storage and release reactions in matching the CO breakthrough behaviour is better assessed by including in the graph the computed level of filling of the total washcoat's oxygen storage capacity. The model shows that CO breakthroughs could be ascribed to empty oxygen storage capacity. In some cases these breakthroughs are successfully predicted (e.g. 350 and 550s) while in other cases (e.g 280 and 470s) are outlined. It must be mentioned that during the periods following the light-off the tailpipe emissions for CO are 50ppm or less that is close to 99% efficiency of the catalyst.

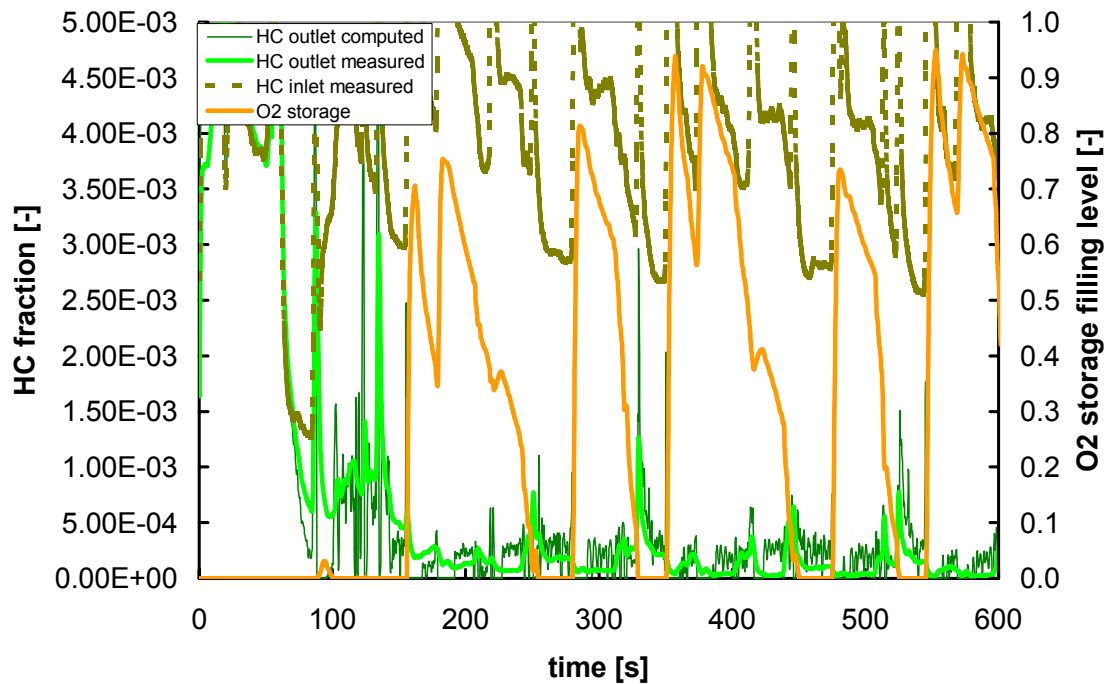


Figure 4 Measured versus computed instantaneous tailpipe HC emissions for the case of 10g/ft³ PML catalyst on NEDC. Bold lines: measured, thin lines: computed

The same situation appears in Figure 4, where the computed and measured instantaneous HC emissions at converter inlet and exit during the first 600 seconds of NEDC are given. The connection between HC breakthroughs and oxygen storage phenomena in the washcoat is apparent also here. HC light-off behavior is also matched with a good accuracy. In HC comparison graphs must be taken into account that in real exhaust gas there are thousands of HC species and current modelling approach assumes only two of them. The shape of the computed curves fits the experimental data and outlines the general behavior of the specific catalytic converter concerning the hydrocarbons.

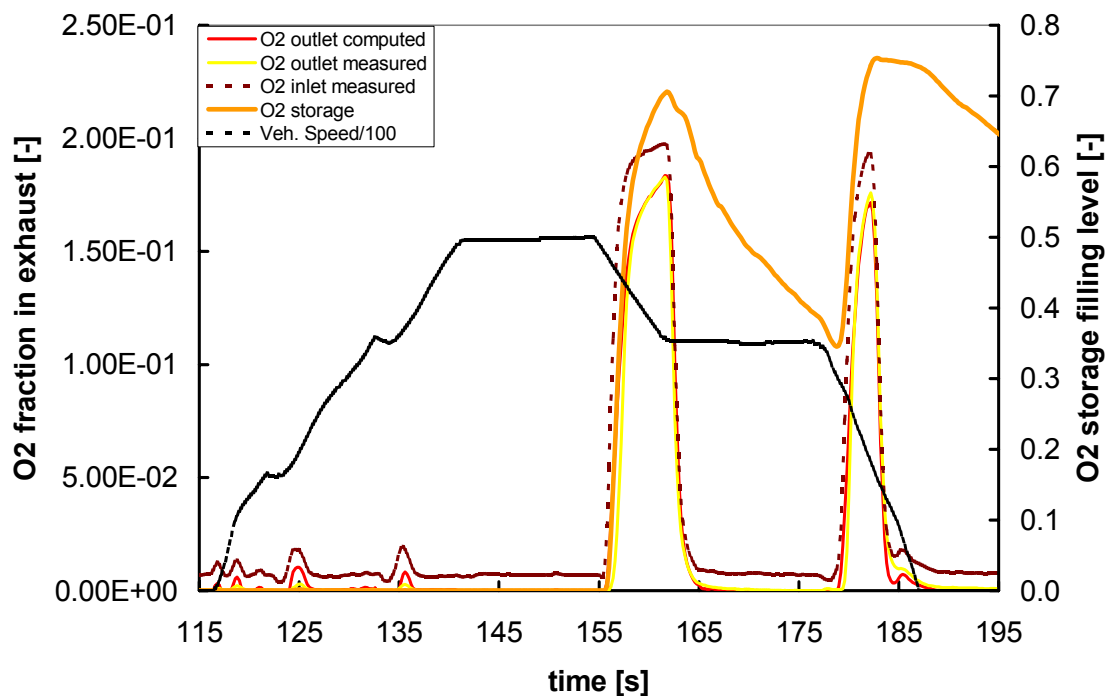


Figure 5 O₂ curves estimation for the case of 10g/ft³ PML catalyst on NEDC. Bold lines: measured, thin lines: computed

Tailpipe oxygen graphs are worth for validation of the oxygen storage capacity estimation. Here it was selected to show the period 115-195s where the oxygen storage completely fills for the first time following a medium acceleration where the engine operates in fuel rich side. The rest of the catalyst outlet measured data for oxygen is close to 100% efficiency. The OSC that was selected seems to be in agreement with the real one, as the peaks of the computational and outlet measured curves are fitted very well during vehicle decelerations when there is a fuel-cut.

6 EFFECT OF PRECIOUS METAL LOADING ON KINETICS

Common questions that could arise during the design of a catalytic converter are which portion of the exhaust gas reacts on each precious metal and what is the contribution of each way of heterogenous catalysis (redox and storage) in three-way catalytic converters. Although these questions can only be answered semi-empirically, based on a large experimental database, modelling is able to assist the designer also in this respect. The study of the contribution of each reaction is of great importance as it can estimate the reasons for defective performance of the converter during operation (breakthrough of the emissions) and study the optimum use of precious metal loading in the washcoat of the catalytic converter.

The oxygen storage level of the catalyst is commonly used by the control system designers [24],[27]. Oxygen distribution among the different reactants shown in Figure 6 can spot cases with oxygen deficiency and assist control improvements. Additionally, estimations of species distribution on the noble metals and Cerium oxides can assist the design of the converter and give some basic directions and feedback to the most fundamental level of modelling and experimental research area. The graphs of Figs 6-8 can demonstrate the computed activity of each catalyst component during NEDC operation. The computed results suggest that the majority of O₂ is reacting primarily with CO (that has the largest concentrations in the exhaust gas) and secondarily with the rest of the gases. A small portion of oxygen should be stored in Cerium oxides, while during extremely lean mixture conditions (e.g. fuel cut) the oxygen present in the exhaust gas should be used to fill the OSC. Similar behavior has been predicted by the kinetic parameters estimated for the case of 10g/ft³ catalyst as shown in Figure 6. “Fast” hydrocarbons species are expected to react primarily on Pt and secondarily with Cerium oxides, as it is described by Figure 7, while “slow” ones are assumed to react only with Pt as previously mentioned. Under rich operation environment (lack of oxygen in the

exhaust gas) HC oxidation is driven with oxygen stored in Cerium oxides and after an oxygen storage fill (e.g. on 550s) hydrocarbons are strongly enhanced by the CeO_2 . According to the previous discussion CO reacts in a similar to the hydrocarbons way. It is mainly oxidised by O_2 over Pt and NO over Rh, while in rich environments it reacts with the stored O_2 in Cerium oxides.

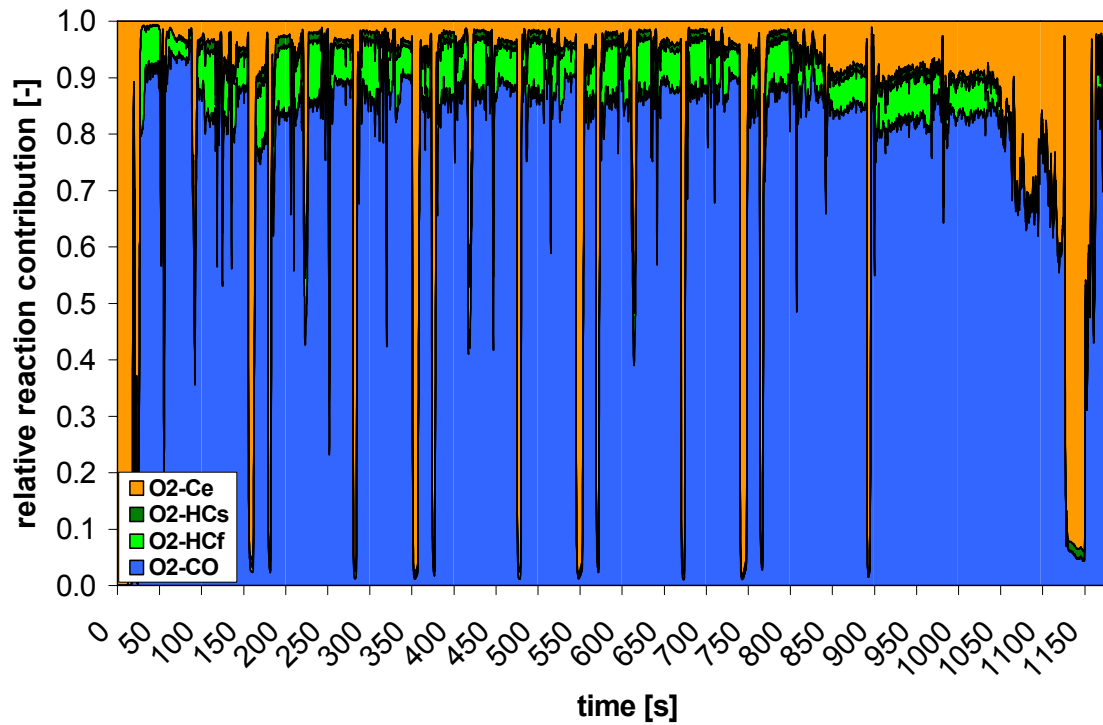


Figure 6 Exhaust oxygen distribution on reactions with exhaust gases and Ce (10g/m3)

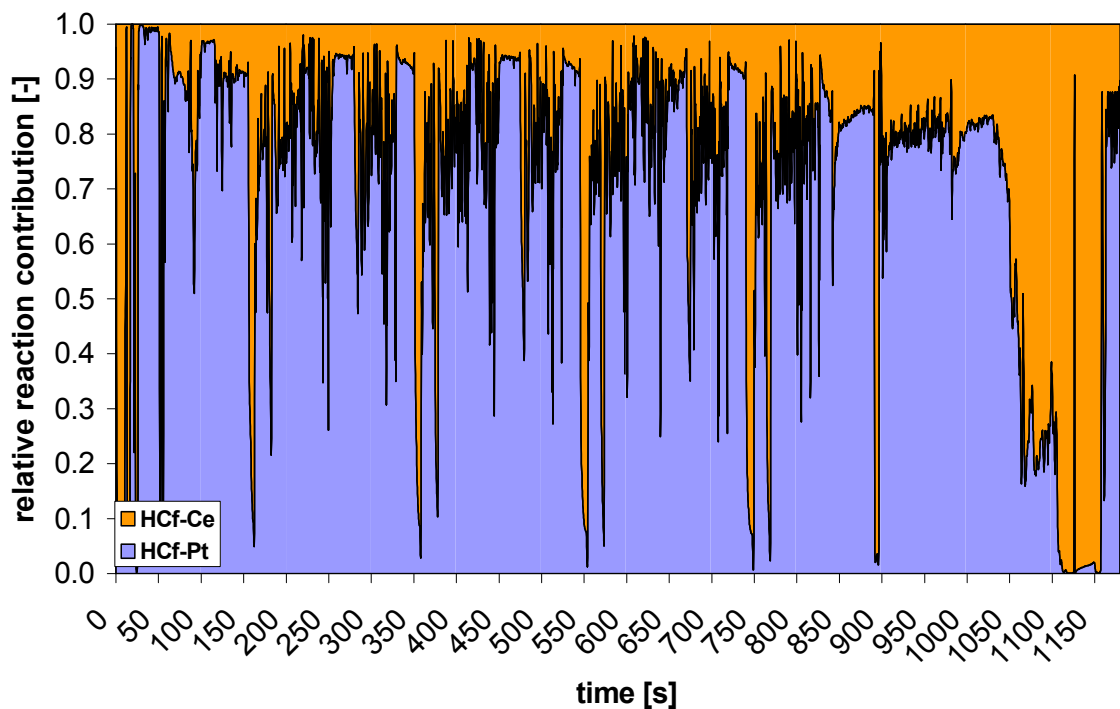


Figure 7 Exhaust HC distribution on PM and Ce

7 EXTRACTION OF A TREND FOR PML EFFECT ON KINETICS

After completion of the respective tuning of the remaining catalysts' performance with the genetic algorithm, the kinetic parameters values estimated by the GA are compared in Figure 8. The performance measure values for

all genetic algorithm runs were of the order of 0.94-0.95, which is considered adequate, also based on the inspection of comparative diagrams.

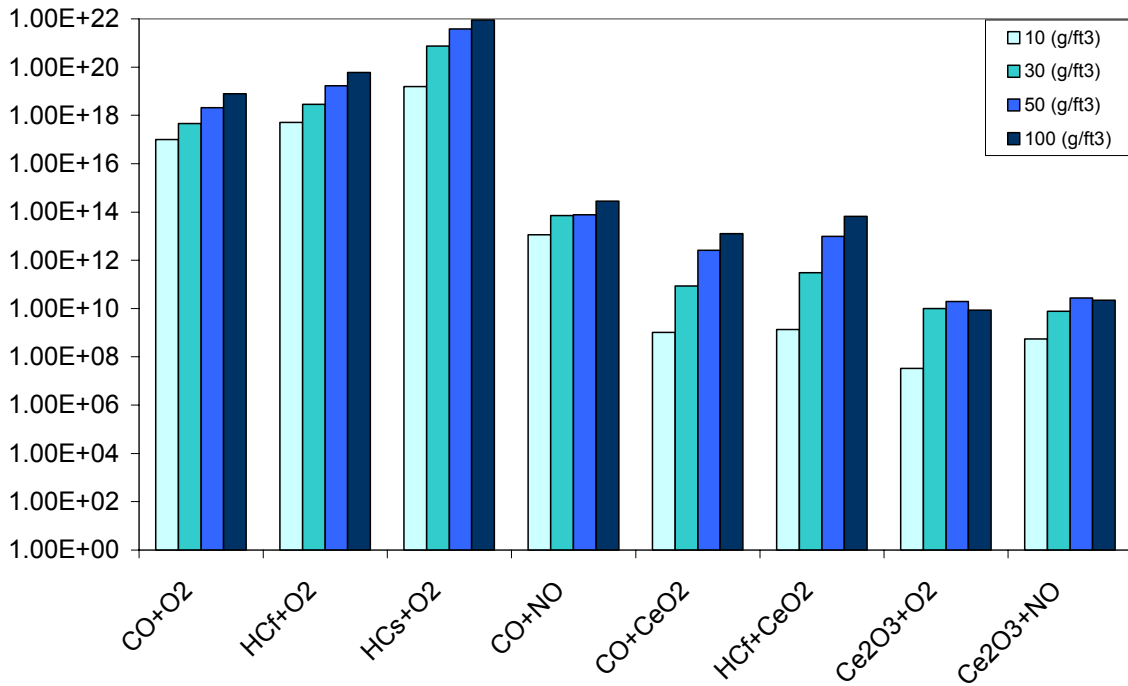


Figure 8 Comparison of predicted kinetic parameters for the case of different PML

It is expected that the catalytic converter must become more active with increase of PML, thus the tunable kinetic parameters of the model should be increased. In general it seems that there is an exponential dependency for the kinetic parameters of the oxidation reactions in respect to the PML, both on precious metals and cerium oxides. The reduction reaction seems to weakly respond on the increase of PML, while oxygen storage filling reactions seem not correlated. Finally the catalyst with the lowest precious metal loading is by far the weakest regarding both redox and storage reactions. Figure 9 and Figure 10 present the estimated kinetic parameters evolution versus population for the case of 10 and 50 g/ft³ catalysts. It is obvious from these figures that the genetic algorithm converges to an optimum area of solutions even at 50th generation. The individuals that are not converged, are ascribed to a built-in subroutine for avoiding local maxima that drives a small portion of the population to search for optimum solutions in the whole space.

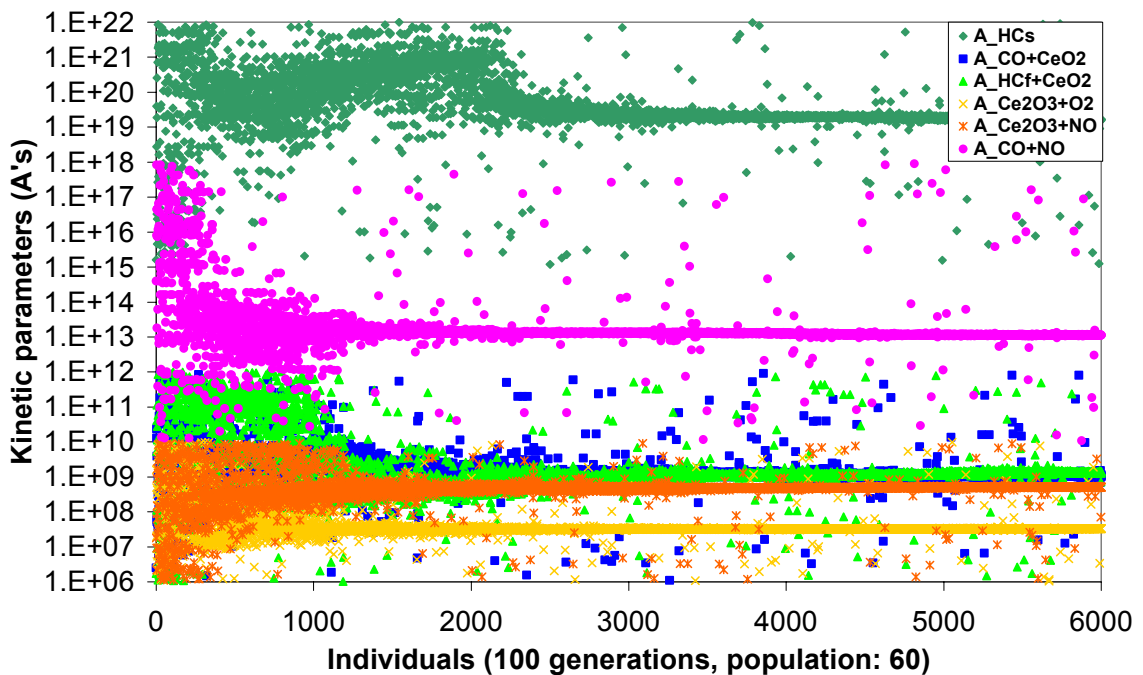


Figure 9 Evolution of genetic algorithm population for the case of 10g/ft³ catalytic converter

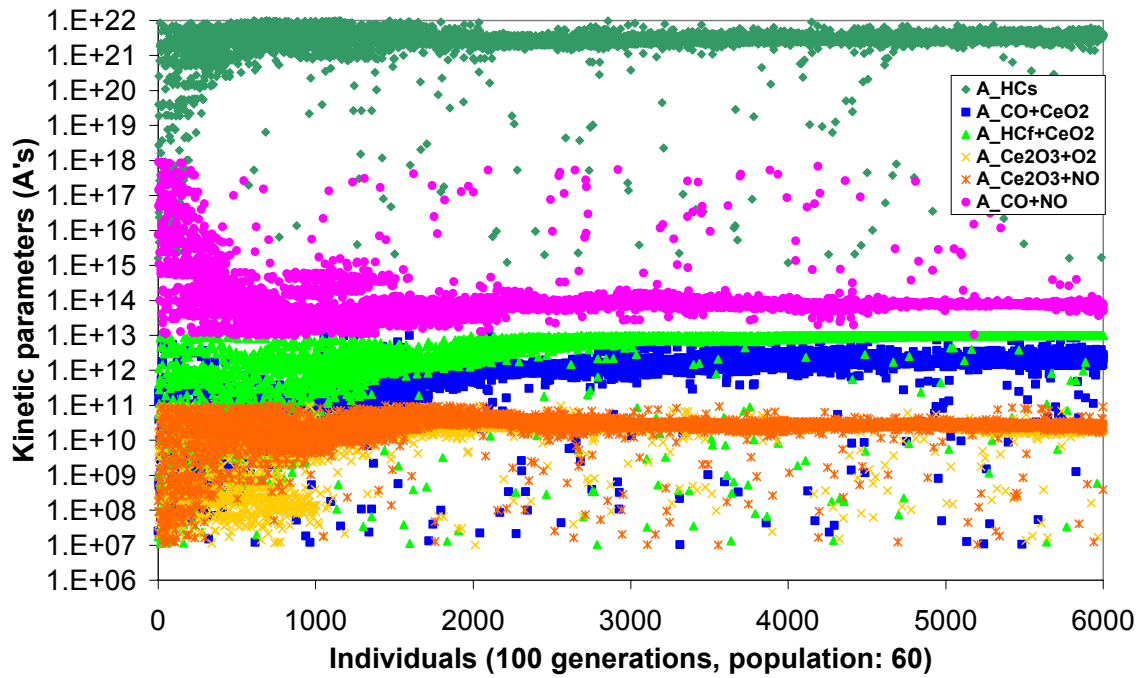


Figure 10 Evolution of genetic algorithm population for the case of 50g/ft³ catalytic converter

Finally, we point out that the evolution of 100 generations of 60 individuals with the genetic algorithm tool lasts about 23 hours on a Pentium IV 2.4Ghz 512Mb RAM and the 3WCC model needs about 14 seconds to simulate the 1180s of the complete NEDC.

8 CONVERTER LENGTH OPTIMIZATION

The tuned kinetic parameters of the 50gr/ft³ catalyst are next employed to computationally study the effect of catalyst length. As a validation case we will use the experimental results of ¼ length catalyst and the full-scale catalyst, both loaded with 50gr/ft³ Pt/Rh 7:1.

Apparently the model is able to predict the length effect of the catalyst also in the case of ¼ length by fitting primarily HC and CO emissions in acceptable limits. Unsuccessful predictions can be attributed to 3D effects concerning that this is a very short catalyst and the uniform flow assumption at converter inlet. As shown in Figure 11 model is able to predict in acceptable limits the behavior of the shorter catalytic converter.

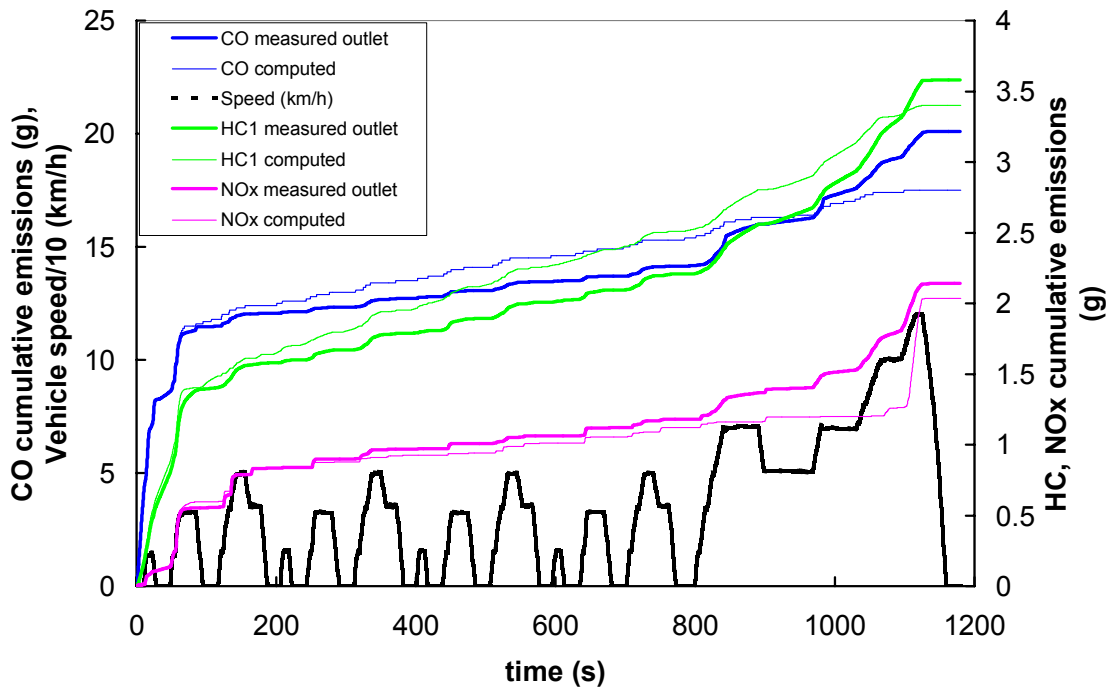


Figure 11 cumulative emissions of ¼ full-scale length of a catalyst loaded with 50gr/ft³ PM

Figure 12 presents the average efficiencies of CO and HC during NEDC for different lengths of catalyst using the same kinetic parameters tuned for the case of 50gr/ft³ catalytic converter. Apparently there is a maximum length for the converter that further increase does not practically improve its efficiency.

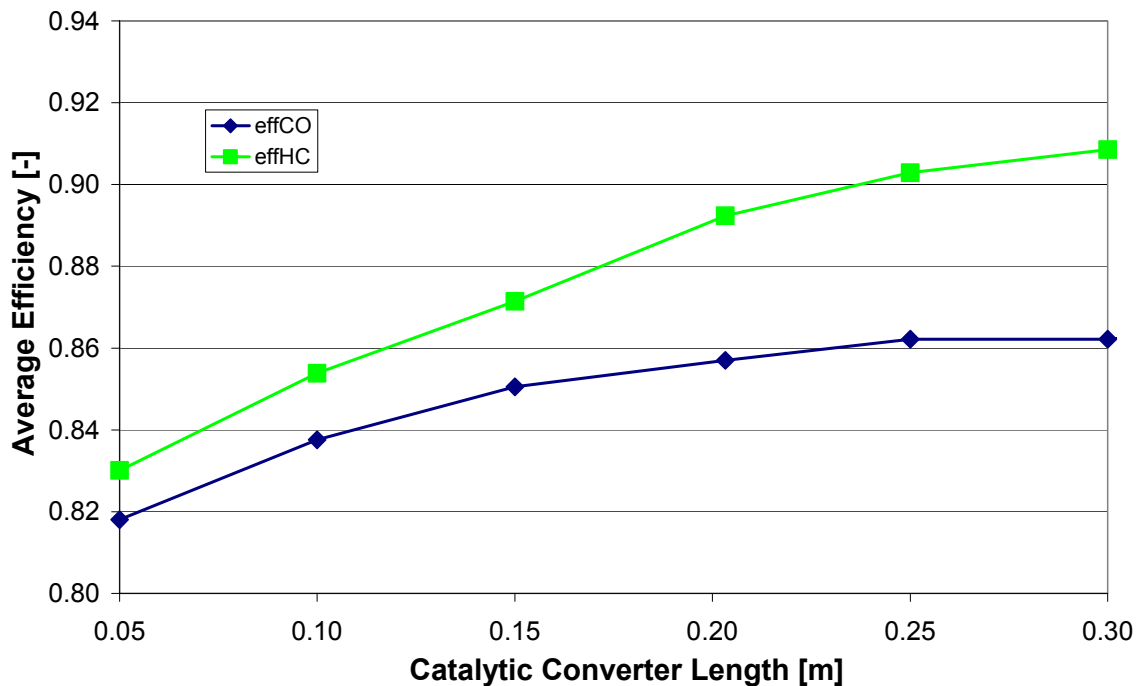


Figure 12 Converter length study results

9 CONCLUSIONS

This paper addresses the application of modern optimisation tools in automotive catalytic converter modelling and design optimization.

The results presented from a demanding computational case study with varying precious metal loading suggest that we can reach a high accuracy in performance prediction by combining a sound engineering model of catalytic converter operation with a parameter estimation tool based on genetic algorithms.

Since a number of catalytic converter model kinetics parameters are tuned based on standard emissions test results, a measurement data quality assurance methodology was essential in the success of the case study.

Apart from the effect of standard design parameters like converter size and positioning, the combination of the above tools now enables to take into account the effect of precious metal loading on the kinetics of the converter's catalytic activity.

Based on the above tools we can proceed in catalytic converter design optimisation, to further improve catalyst performance with minimized additional production cost.

Acknowledgements

The authors would like to thank Dr. G. Pontikakis who wrote the code of the genetic algorithm tool. The financial support of author G. Konstantas by the Greek State Scholarships Foundation is gratefully acknowledged

REFERENCES

- ¹ Oh, S. H. and Cavendish, J. C. (1985). Mathematical modeling of catalytic converter light-off – Part III: Prediction of vehicle exhaust emissions and parametric analysis. *AIChE Journal*, 31 (6).
- ² Stamatelos, A.M.; Koltsakis, G.C., I.P. Kandyas (1999). Computergestützte Entwurf von Abgasnachbehandlungssystemen. Teil I. *Ottomotor Motortechnische Zeitschrift*, 60, 2, 116-124.
- ³ Koltsakis, G.C.; Konstantinidis, P.A.; Stamatelos A.M. (1997). Development and Application Range of Mathematical Models for Automotive 3-Way Catalytic Converters. *Applied Catalysis B Environmental*, 12, Issue 2–3, 161–191
- ⁴ Chen, D.K.S.; Bisset, E.J.; Oh, S.H. and Van Ostrom, D.L. (1988). A three-dimensional model for the analysis of transient thermal and conversion characteristics of monolithic catalytic converters. *SAE paper 880282*
- ⁵ Braun, J.; Hauber, T.; Taobben, H.; Windmann, J.; Zacke, P.; Chatterjee, D.; Correa, C.; Deuchmann, O.; Maier, L.; Tischer, S. and Warnatz, J. (2002). Three-dimensional simulation of the transient behaviour of a three-way

catalytic converter. SAE paper 2002-01-0065.

⁶ Pontikakis, G.N. and Stamatelos, A.M. (2001). Mathematical Modeling of Catalytic Exhaust Systems for EURO-3 and EURO-4 Emissions Standards. Proc. Inst. Mech. Engrs., Part D, Journal of Automobile Engineering, Vol 215, 1005-1015

⁷ Pontikakis, G.N.; Konstantas, G.S. and Stamatelos, A.M. (2003). Three-way Catalytic Converter Modelling as a Modern Engineering Design Tool, ASME Transactions, Journal of Engineering for Gas Turbines and Power

⁸ Konstantas, G.S. and Stamatelos, A.M. (2004). Quality Assurance of Exhaust Emissions Test Data. In Press, Proc Instn Mech Engrg Part D: J Automobile Engineering

⁹ LTTE–University of Thessaly: CATRAN Catalytic Converter Modeling Software. User’s Guide, Version v4r2f. Volos, June 2003.

¹⁰ Siemund, S.; Leclerc, J. P.; Schweich, D.; Prigent, M. and Castagna, F. (1996). Three-way monolithic converter: simulations versus experiments. Chem. Eng. Sci., 51, (15), 3709–3720.

¹¹ Chen, D.K.S.; Bisset, E.J.; Oh, S.H. and Van Ostrom, D.L. (1988). A three-dimensional model for the analysis of transient thermal and conversion characteristics of monolithic catalytic converters. SAE paper 880282

¹² Voltz, S.E.; Morgan, C.R.; Liederman, D.; Jacob, S.M. (1973). Kinetic study of carbon monoxide and propylene oxidation on platinum catalysts. Ind. Eng. Chem. Prod. Res. Dev. 12, 294.

¹³ Zygourakis, K. and Aris R. (1983). Multiple oxidation reactions and diffusion in the catalytic layer of monolith reactors. Chem. Eng. Sci, 38 (5), 733–744

¹⁴ Keren, I.; Sheintuch, M. (2000). Modeling and analysis of spatiotemporal oscillatory patterns during CO oxidation in the catalytic converter. Chem. Eng. Sci., 55, 1461–1475.

¹⁵ Zhdanov, V.P. and Kasemo, B. (1998). Kinetic models of oxygen supply from CeO_x to active nanometer particles of three-way catalysts. Applied Surface Science 135, 297–306

¹⁶ Botas, J.A.; Gutiérrez-Ortiz, M.A.; González-Marcos, M.P.; González-Marcos, J.A. and González-Velasco, J.R. (2001). Kinetic considerations of three-way catalysis in automobile exhaust converters Applied Catalysis B: Environmental 32, 243–256

¹⁷ Pontikakis, G.N. (June 2003) Modeling, Reaction Schemes and Parameter Estimation in Catalytic Converters and Diesel Filters. PhD Thesis, Mechanical Engineering Dept., University of Thessaly, Volos, (http://www.mie.uth.gr/labs/lte/pubs/PhD_G_Pont.pdf)

¹⁸ Pontikakis, G.N. and Stamatelos, A.M. (2003). Identification of Catalytic Converter Kinetic Model Using a Genetic Algorithm Approach. Submitted, Proc Instn Mech Engrg Part D: J Automobile Engineering

¹⁹ Lindner, D., Mussmann, L., Van den Tillaart, J.A.A., Lox, E.S., Roshan, A., Garr, G., Beason, R. (2000) Comparison of Pd-only, Pd/Rh, and Pt/Rh Catalysts in TLEV, LEV Vehicle Applications – Real Vehicle Data versus Computer Modeling Results, SAE paper 2000-01-0501

²⁰ Votsmeier, M., Bog, T., Lindner, D., Gieshoff, J., Lox E.S., Kreuzer T. (2002). A System(atic) Approach towards Low Precious Metal Three-Way Catalyst Application. SAE paper 2002-01-0345.

²¹ Lox, E.S. (2003): "State of the art methods for the development of automotive catalysts", CAPOC6 Keynote

²² Manilla, P.; Salmi, T.; Haario, H.; Luoma, M.; Harkonen, M.; Sohlo, J. (1996). Stationary kinetics of essential reactions on automobile exhaust Pt-Rh/Al₂O₃ catalyst, Applied Catalysis B: Environmental 7, 179-198

²³ Glielmo L. and Santini S. (2001). A Two-Time-Scale Infinite-Adsorption Model of Three Way Catalytic Converters During The Warm-Up Phase, Journal of Dynamic Systems, Measurement and Control, Transactions of the ASME, vol.123, 62-70

²⁴ Aimard, F.; Li, S. and Sorine M. (1996). Mathematical Modeling Of Automotive Three-Way Catalytic Converters With Oxygen Storage Capacity, Control Eng. Practice, Vol. 4, No8, pp.1119-1124

²⁵ Theis, J.R. (1996). An engine Test to Measure the Oxygen Storage Capacity of a Catalyst, SAE paper 961900

²⁶ Kandylas, I.P.; Stamatelos, A.M. and S.G. Dimitriadis (1999). Statistical Uncertainty in Automotive Emissions Testing Proc. Inst. Mech. Engrs., Vol.213, Part D, J. of Automobile Engineering, 491-502.

²⁷ Shafai, E.; Roduner C. and Geering, H.P. (1996) Indirect Adaptive Control of a Three-Way Catalyst, SAE paper 961038